Structural characterisation of melt-spun Ti$_{50}$Ni$_{25}$Cu$_{25}$ ribbons

D. Schryvers, P.L. Potapov, A. Ledda and A.V. Shelyakov[1]

Electron Microscopy for Materials Research (EMAT), University of Antwerp, RUCA, Groenenborgerlaan 171, 2020 Antwerp, Belgium
[1] *Moscow Engineering Physics Institute, Kashirskoe Shosse 31, 115409 Moscow, Russia*

Abstract. The structure of melt-spun Ti$_{50}$Ni$_{25}$Cu$_{25}$ ribbons after various heat treatments has been studied by X-ray and TEM analyses. As-received amorphous Ti$_{50}$Ni$_{25}$Cu$_{25}$ ribbons, when annealed at 500^{0}C for a few minutes, crystallise into the B2 structure, which fully transforms into the orthorhombic martensite upon cooling. The X-ray scans of Ti$_{50}$Ni$_{25}$Cu$_{25}$ ribbons annealed for 5 min. at 500^{0}C show the well developed orthorhombic pattern, which was used for refinement of the orthorhombic martensitic structure of TiNi-Cu alloys. The refined structure of the orthorhombic martensite in TiNi-Cu alloys differs from the standard B19 type suggested previously. X-ray investigation reveals a shift of atoms in the (0$\bar{1}$0)$_{ORT}$ layers from the centro-symmetric positions towards the [001]$_{ORT}$ direction. The longer annealing of Ti$_{50}$Ni$_{25}$Cu$_{25}$ ribbons at 500^{0}C causes TiCu precipitation and results in appearance of untransformed B2 grains at room temperature. Annealing at 700^{0}C causes Ti$_3$Cu$_4$ precipitation with significant Cu depletion of the matrix resulting in the appearance of the mixed orthorhombic and monoclinic martensite.

1. INTRODUCTION

TiNi-based shape memory alloys attract much attention for their unique properties associated with the reversible martensitic transformation. Although the addition of third elements typically cancels the shape memory effect, the addition of up to 30% of Cu has been shown to retain shape memory properties [1,2]. Due to the evident importance of ternary alloys, several authors have characterised their structure [2-5, 7-10], although, still now, the structural state of TiNi-Cu is much less documented than that of binary TiNi. It has been demonstrated [3] that alloys consisting of more than 10% Cu transform from the parent cubic to the martensitic orthorhombic structure. Fig.1 shows a schematic of the transformation [6] from the parent B2 structure to the orthorhombic martensitic structure. The transformation involves deformation of the parent structure along [001]$_{B2}$, [110]$_{B2}$ and [1$\bar{1}$0]$_{B2}$ directions followed by a (110)[1$\bar{1}$0]$_{B2}$ shuffle. The lattice deformations were examined by Nam et al. [3] though the magnitude of the shuffle, denoted as δ in Fig.1, was never measured experimentally. The effect of heat treatment on the structure of TiNi-Cu alloys is even less studied. Available papers [9,10] report the formation of coherent TiCu precipitates on ageing at the temperature range of 400...700^{0}C. This precipitation process affects strongly the structural situation in TiNi-Cu alloys resulting in a change of microstructure [9] and an occurrence of a multi-stage martensitic transformations [10]

Nowadays, the technique of rapid solidification of TiNi-Cu alloys becomes available allowing fabrication of homogeneous material with a high Cu-content [11]. Such melt-spun TiNi-Cu alloy can be obtained in high quality thin ribbons suitable for accurate structural examinations. This paper presents a structural characterisation of Ti$_{50}$Ni$_{25}$Cu$_{25}$ melt-spun ribbons after various heat treatments. The structural details are examined at different length scales from the microscopic to atomic level.

2. EXPERIMENTAL

Amorphous ribbons containing 50 at.% Ti, 25at.%Ni and 25at.%Cu, were manufactured by the single-roller melt-spinning technique under argon atmosphere. The spinning yields a cooling rate of about 5x10^5 K/s. Then, the ribbons were subjected to a heat treatment at temperatures varying from 500^{0}C to 700^{0}C in evacuated quartz tubes or in-situ in a column of an electron microscope.

The TEM studies were performed on a Philips CM-20 twin microscope operating at 200kV equipped with a Si(Li) Oxford EDX detector and a heating holder. X-ray diffraction studies were performed in the Bragg-Brentano geometry using a powder Philips PW1830 diffractometer with monochromated Cu K$_\alpha$ radiation. The Rietveld-refinement program RIETAN-98 developed by F. Izumi (NIRIM, Tsukuba, Japan) was used for refinement the crystal structure of martensite. The preferred orientation was described by the Marsh-Dollase function[12] with the adjustable parameter r, which should be less than 1 when preferred orientations exist.
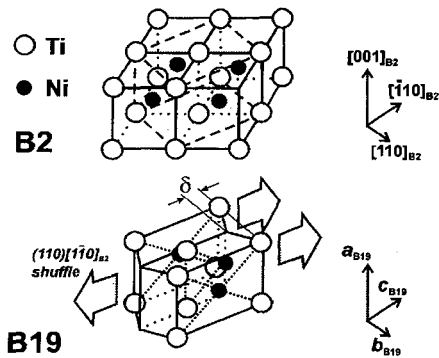

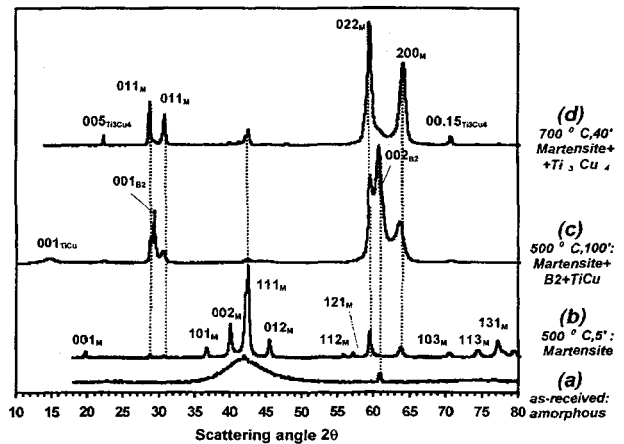**Figure 1** Schematic of the structural transformation from B2 to B19 after Otsuka and Ren [6].

Figure 2 Room temperature X ray scans of TiNi-Cu ribbons after different heat treatments.

3. RESULTS AND DISCUSSION

3.1 Structural Evolution in Ni$_{25}$Ti$_{50}$Cu$_{25}$

Fig.2 shows room temperature X-ray scans of Ti$_{50}$Ni$_{25}$Cu$_{25}$ ribbons after various treatments. As-received melt spun ribbons are amorphous (Fig.2a) and show good chemical homogeneity as proved by EDX examination. The average composition was measured as 51.2at.%Ti, 25.2at.%Ni and 23.6at.%Cu. In-situ annealing in an electron microscope at 500°C for several minutes reveals crystallisation into the B2 structure, which undergoes the martensitic transformation when returning to room temperature. Ribbons annealed at 500^{0}C for 5min. show a single pattern of the orthorhombic martensitic structure (Fig.2b). The fine crystal structure of the martensite will be analysed in details in the next section. Longer annealing at 500^{0}C (Fig.2c) results in a strong preferential orientation of the orthorhombic martensite, i.e. orientation of (011)$_{ORT}$ and (100)$_{ORT}$ planes preferentially along the normal to the casting plane. These two preferred orientations evidently originate from the 100 texture of the parent B2 phase formed at 500^{0}C [10]. According to the orientation relationship between the parent and martensitic structures shown in Fig.1, the {100}$_{B2}$ planes transform into (011)$_{ORT}$ and (100)$_{ORT}$ planes on cooling. Also, some amount of untransformed B2 structure is observed with a volume fraction raising with increasing the annealing time. Simultaneously, X-ray examination detects the appearance of the 001 peak belonging to the B11 tetragonal structure of the TiCu compound [13]. Other typical peaks for this compound are masked by the strong peaks from the orthorhombic martensite. These results correlate with the previous works reporting precipitation of TiCu in Ti$_{50}$Ni$_{25}$Cu$_{25}$ alloys annealed for a few hours at 500^{0}C [10]. The existence of the retained B2 phase and thegrowth of TiCu precipitates at 500^{0}C could be the related processes, as precipitation changes locally the composition of the matrix and can, thus, alter the local temperature for martensitic transformation. An alternative explanation suggested by Rösner et al.[10] involves structural hampering the transformation by thin plate-like TiCu precipitates coherent with the B2 matrix.

Annealing at 700°C also induces the preferential orientation of the martensite (Fig.2d), however, without the formation of the retained parent phase. The strong 011 and 100 textures do not allow to determine whether the martensite is orthorhombic or monoclinic. In contrast to the treatment at 500°C, no 001 peak from the TiCu phase was detected. Instead, as seen in Fig.2d, two peaks at 22 and 71 deg. appear, suggesting precipitation of a new phase. These peaks could be indexed as the 005 and 0015 lines of the tetragonal Ti_3Cu_4 structure [14]. The limited amount of the observed peaks does not allow, however, to perform a comprehensive X-ray analysis of the new phase.
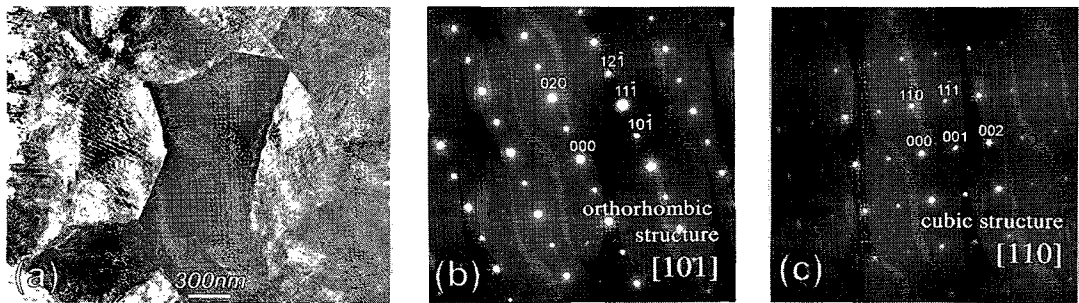

Figure 3 (a) Typical microstructure of TiNi-Cu ribbon treated at 500°C for 5 min. with a SAED pattern of **(b)** orthorhombic martensite and **(c)** untransformed cubic structure.

TEM reveals the further details of structural evolution of $Ti_{50}Ni_{25}Cu_{25}$ during various heat treatments. Fig.3a shows the microstructure of a TiNi-Cu ribbon annealed at 500°C for 5 min. In agreement with the X-ray results, the material was found to be crystallised with grains of 0.5-1um in size. Almost all grains are transformed to the orthorhombic martensite and demonstrate the fine internal twinning typical for martensitic phases. Fig.3b shows a SAED pattern, which can be indexed as the 101 zone of the orthorhombic martensite. Occasionally, few untransformed grains with the cubic structure are found already after treatment for 5 min at 500°C. The SAED pattern of the cubic structure along the 110 zone shows the B2 type ordering with 001 superstructural reflections (Fig.3c). No additional reflections at positions corresponding to L2₁ or DO₃ types of ordering were detected. Thus, Cu atoms seem to be randomly distributed in the Ni-sublattice retaining the B2 type order as in binary TiNi. An increase of the annealing time results in appearance of fine precipitates and forming more untransformed B2 grains.
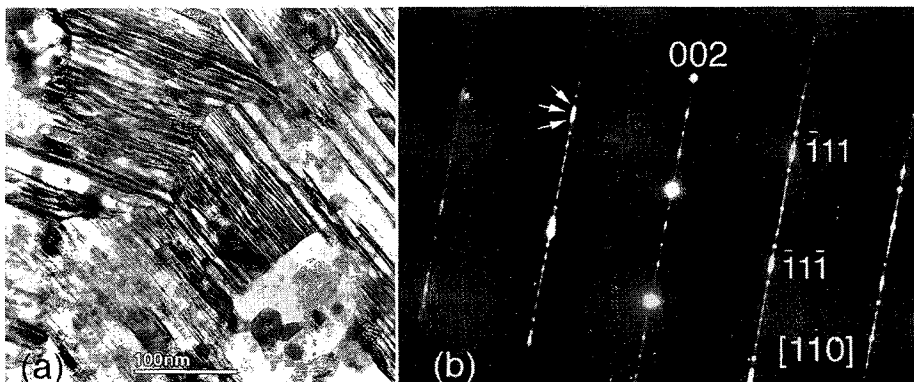

Figure 4 (a) Martensite plates formed on cooling after annealing at 700°C and **(b)** SAED pattern revealing a mixture of the orthorhombic and monoclinic martensites. The pattern is indexed in the $[110]_{ORT}$ zone while arrows indicate satellites around each orthorhombic reflection due to the formation of the two variants of the monoclinic martensite.

When increasing the annealing temperature to 700°C, larger precipitates appear in the B2 matrix. Upon cooling, as observed by in-situ TEM observations, the B2 structure transforms to a twinned martensitic (Fig.4a) structure at temperatures varying spatially over the matrix. In some regions, the transformation occures around 300°C, i.e. at a much higher temperature then normally observed in TiNi-based alloys. The variation of the local composition caused by precipitation was examined by EDX. The average composition of precipitates was measured as 54.3at.%Cu, 38.1at.%Ti and 7.5at.%Ni, which supports their identification as the Ti_3Cu_4 phase. The Cu-content in the matrix varied from 7 to 14at.% suggesting that the martensite is no longer orthorhombic but could consist of a mixture of orthorhombic and monoclinic structures. Indeed, the diffraction pattern observed near the fine martensitic plates (Fig.4b), can be explained by a mixture of the [110] zone of the orthorhombic B19 structure and two variants of the monoclinic B19'. In the latter, the twinning occurs on the (001) planes, which can be related with a compound twin mode reported in binary NiTi [6].

3.2 Refinement of Martensite Structure in $Ni_{25}Ti_{50}Cu_{25}$

The orthorhombic martensitic structure in TiNi-Cu alloys has been suggested to be the B19 structural type, determined in TiPt, TiPd, MgCd and TiAu [15] and known to belong to the *Pmmb* space group. Identification of TiNi-Cu martensite as the B19 structure is based mainly on geometrical considerations as in Fig.1, which dictate the *Pmmb* group for the resulting orthorhombic structure. However, this group is not limited to the given B19 structure type. As shown in Fig.5, the B19 structure implies a centre of symmetry in the $(010)_{ORT}$ atomic layers while the *Pmmb* group generally allows a shift of Ni atoms from the central position in the $[001]_{ORT}$ direction. To keep the *Pmmb* symmetry group, this shift should alternate its direction in each subsequent $(010)_{ORT}$ layer. To distinguish with the B19 type, the resulted structure will be referred as 'orthorhombic' with an index 'ORT'. Such an atomic shift can be described as a transverse wave of the Ni sublattice with a wave vector $[110]_{B2}$, a shift direction $[\bar{1}10]_{B2}$ and an amplitude v, where the v-value is depicted in Fig.1b. Note that two distinguished directions of a v shift are possible: in phase or antiphase with respect to the shuffle direction of δ. The former will be denoted as positive and the latter as negative v. The possibility of such a shift was never considered in TiPt, TiAu, MgCd alloys with the reported B19 structure, because the maximal symmetry of $(010)_{ORT}$ layers was always assumed [15]. Such an assumption, however, does not appear straightforward for TiNi-Cu, as an asymmetric configuration of the $(010)_{B19'}$ layers has already been discovered in the B19' structure of binary TiNi [16,17]. Additionally, a small shift of atoms from the central-symmetric positions has been observed in the $(010)_{ORT}$ layers of the orthorhombic AuCd [9], which was previously considered as having the B19 type [18].

Table 1 lists the results of the Rietveld refinement of atomic positions with several hypotheses. Additionally, the degree of order and the thermal displacement factor were varied although they show only a small influence on the reliability factor R. Assumption of a v-shift in the $(010)_{ORT}$ layers as depicted in Fig.5, improves the R factor noticeably. The best match with experiment is obtained at a shift value of about 2.5% of the c parameter. Further improvement can be obtained by taking the preferred orientation of grains into account. Table 1 lists two types of texture, 011 and 010, which were found to improve the R factor. Assumption of the 010 texture yields the best results. However, despite of the good R number, the Rietveld method has the intrinsic problem with the correct accounting of the preferred orientation in martensitic polycrystals. As known from the crystallography of the cubic→orthorhombic martensitic transformation, each single orientation of the parent phase transforms into at least 12 orientation variants of the orthorhombic phase [15]. Even taking in consideration that some of these variants are crystallographically equivalent, the simply textured B2 must cause several preferred orientations in the product orthorhombic phase. That was, indeed, confirmed in the samples annealed at 700°C (see Fig.2d). Accounting such several preferred orientation is difficult for the Rietveld method.
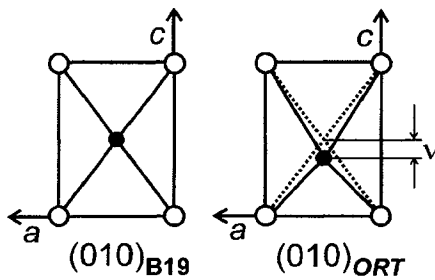
Figure 5 The atomic configuration of (010) layers in B19 and the general *Pmmb* space group.
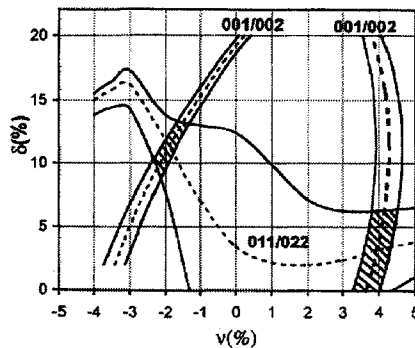
Figure 6 Lines in the 2D δ-v space satisfying the experimental intensity ratios between 001/002 and 011/022 peak couples. Each line is presented including the borders showing the actual experimental precision.

Table 1. Results of Rietveld refinement of atomic positions in the orthorhombic TiNi-Cu martensite.

Assump-tion of v shift	Preferred orientation vector	R	Refined parameters				
			Preferred orientation parameter r	Shuffle δ	Shift v	Degree of order	Thermal atomic displacement
NO	NO	4.33%	-	5.0%	-	0.96	0.46
YES	NO	3.98%	-	5.1%	-2.6%	0.98	0.35
YES	011	3.80%	0.89	4.9%	-2.8%	0.95	0.46
YES	010	3.10%	0.89	5.1%	-2.4%	0.99	0.44

To avoid unpredictable influence of the preferred orientations, we performed a selective analysis of couples of reflections located along the same crystallographic directions. The intensity ratio between 100/200, 001/002 and 011/022 peaks was measured as 0.083 ± 0.045, 0.117 ± 0.021 and 0.080 ± 0.023, respectively and these ratios should not be sensitive to the texture of the sample. The 100/200 ratio depends only on the order between Ti and Ni sublattices and the measured value of 0.083 yields a degree of order of 0.90 ± 0.12. The 001/002 and 011/022 ratios are strongly sensitive to the z-positions of both Ti and Ni atoms. Fig.6 plots the lines in the 2D δ-v space, which satisfy the experimental 001/002 and 011/022 values including the actual experimental precision. Note that two different lines with positive and negative v both satisfy the measured 001/002value of 0.117. The crossing of the 001/002 and 011/022 lines yields two possible (δ, v) solutions matching the experimental 001/002 and 011/022 ratios. The solution with $\delta=3.5\%$ and $v=+3.9\%$ is rejected, because it results in non-consistent intensities of 112, 121, 103, 113 and other peaks with higher 2θ, even accounting for texture. For instance, the calculated intensity of the 103 peak is almost zero, while this peak is clearly seen in Fig.2b. The second solution with $\delta=11.4\%$ and $v=-1.8\%$, gives realistic intensities for peaks with higher 2θ.

So, both the standard Rietveld refinement and selective intensity analysis yield a v value of about -2%. The δ values obtained by both methods differ noticeably (5.1% and 11.4%) which is probably explained by the lower sensitivity of the peak intensities to the δ parameter. The value of 11.4% for δ is retained as the selective intensity analysis is not sensitive to the preferred orientation in the sample. Thus, the present experimental work reveals a shift of atoms inside the $(010)_{ORT}$ layers of the orthorhombic TiNi-Cu martensite, although the reason for appearance of such a shift is not quite clear. It is unlikely that this shift is related with the ternary composition of $Ti_{50}Ni_{25}Cu_{25}$ alloy, as Cu and Ni atoms seem to be randomly mixed in the Ni-sublattice. Note that the B19'structure in binary TiNi also exhibits atomic shifts from the centro-symmetric positions [16,17] despite of its simple equiatomic composition, thus the atomic configuration of martensitic structures in TiNi and TiNi-Cu could be related with each other [20].

4. CONCLUSIONS

1. As-received amorphous melt-spun $Ti_{50}Ni_{25}Cu_{25}$ ribbons crystallise by a few minutes annealing at 500^0C resulting in the B2 structure, which fully transforms into the orthorhombic martensite upon cooling. Longer annealing at this temperature causes TiCu precipitation and results in retained untransformed B2 grains at room temperature.
2. Annealing of melt-spun $Ti_{50}Ni_{25}Cu_{25}$ ribbons at 700^0C causes Ti_3Cu_4 precipitation with significant Cu depletion of the matrix resulting in the appearance of a mixture of orthorhombic and monoclinic martensite.
3. The structure of the orthorhombic martensite in TiNi-Cu alloys differs from the standard B19 type suggested previously. X-ray investigation reveals a shift of atoms in the $(010)_{ORT}$ layers from the centro-symmetric positions towards the $[001]_{ORT}$ direction.

References

1. O.Mercier and K.N.Melton, Met.Trans.A, **10A**, 387 (1979)
2. H.Nam, T.Saburi and K.Shimizu, Mat.Trans. JIM, **31**, 959 (1990)
3. H.Nam, T.Saburi, I.Nakata and K.Shimizu, Mat.Trans. JIM, **31**,1050 (1990)
4. W.J.Moberly, J.L.Proft, T.W.Duerig and R.Sinclair, Mat.Sci.Forum, **56-58**, 605 (1990)
5. T Y.C.Lo, S.K.Wu and H.E.Horng, Acta Met., **41**, 747 (1993)
6. K.Otsuka and X.Ren, Intermetallics, **7**, 511(1999)
7. V.G.Pushin, S.B.Volkova, N.M.Matveeva, L.I.Yurchenko and A.S Chistyakov, The Phys.Met.&Metallogr., **83**, 673(1997)
8. V.G.Pushin, S.B.Volkova, N.M.Matveeva, L.I.Yurchenko and A.S Chistyakov The Phys.Met.&Metallogr., **83**, 679(1997)
9. V.G.Pushin, S.B.Volkova, N.M.Matveeva, L.I.Yurchenko and A.S Chistyakov, The Phys.Met.&Metallogr., **84**, 441 (1997)
10. H.Rösner,A.V.Sheliakov, A.M.Glezer, K.Feit, P.Schlossmacher,Mat.Sci.Eng.A, **273-275**,733 (1999)
11. N.M.Matveeva, Yu.K.Kovneristy, Yu.A.Bukovsky, A.V.Shelyakov and O.V.Kostyanaya, Izvestia Akad.Nauk SSSR Metalli, **4**, 171 (1989)
12. W.A.Dollase, J.Appl.Cryst., **19**, 267 (1986)
13. Karlson, J.Inst.of Metals, **79**, 391 (1951)
14. Schubert, Z.Metallknde, **56**, 197 (1965)
15. A.E.Dwipht, R.A.Coner Jr. and J.W.Downey, Acta cryst., **18**, 837 (1965)
16. G.M.Michal and R.Singlar, Acta Cryst., **B37**, 1803(1981)
17. Y.Kudoh, M.Tokonami, S.Miyazaki and K.Otsuka, Acta Met., **33**, 2049 (1985)
18. T.Ohba, Y.Emura, S.Miyazaki and K.Otsuka, Mat.Trans. JIM, **31**, 12 (1990)
19. R.D.James, K.F.Hane, Acta Mat., **48**, 197(2000)
20. P.L.Potapov, A.V.Shelyakov and D.Schryvers, to be published in Scripta Mat.